

1 **Title Page**

2

3 **The Proteolytic Landscape of an Arabidopsis Separase-Deficient Mutant Reveals Novel**
4 **Substrates Associated With Plant Development**

5

6 Chen Liu¹, Simon Stael^{2,3,4,5}, , Kris Gevaert^{4,5}, Frank Van Breusegem^{2,3}, Peter V Bozhkov⁶,
7 Panagiotis N Moschou¹

8

9 ¹Department of Plant Biology, Uppsala BioCenter, Swedish University of Agricultural
10 Sciences and Linnean Center for Plant Biology, SE-75007 Uppsala, Sweden

11 ²Department of Plant Systems Biology, VIB, 9052 Ghent, Belgium

12 ³Department of Plant Biotechnology and Bioinformatics, Ghent University, 9052 Ghent,
13 Belgium

14 ⁴VIB-UGent Center for Medical Biotechnology, 9000 Ghent, Belgium

15 ⁵Department of Biochemistry, Ghent University, 9000 Ghent, Belgium

16 ⁶Department of Molecular Sciences, Uppsala BioCenter, Swedish University of Agricultural
17 Sciences and Linnean Center for Plant Biology, SE-75007 Uppsala, Sweden

18

19

20 Corresponding author:

21 Panagiotis N Moschou

22 panagiotis.moschou@slu.se

23 Department of Plant Biology

24 Uppsala BioCenter

25 Swedish University of Agricultural Sciences and Linnean Center for Plant Biology

26 PO Box 7080

27 SE-75007 Uppsala

28 Sweden

29 Tel: +46 700780553

30

31 **Abstract**

32 Digestive proteolysis executed by the proteasome plays an important role in plant development.
33 Yet, the role of limited proteolysis in this process is still obscured due to the absence of studies.
34 Previously, we showed that limited proteolysis by the caspase-related protease separase
35 (EXTRA SPINDLE POLES [ESP]) modulates development in plants through the cleavage of
36 unknown substrates. Here we used a modified version of the positional proteomics method
37 COmbined FRActional DIagonal Chromatography (COFRADIC) to survey the proteolytic
38 landscape of wild-type and separase mutant *RADIALLY SWOLLEN 4* (*rsw4*) root tip cells, as
39 an attempt to identify targets of separase. We have discovered that proteins involved in the
40 establishment of pH homeostasis and sensing, and lipid signalling in wild-type cells, suggesting
41 novel potential roles for separase. We also observed significant accumulation of the protease
42 PRX34 in *rsw4* which negatively impacts growth. Furthermore, we observed an increased
43 acetylation of N-termini of *rsw4* proteins which usually comprise degrons identified by the
44 ubiquitin-proteasome system, suggesting that separase intersects with additional proteolytic
45 networks. Our results hint to potential pathways by which separase could regulate development
46 suggesting also novel proteolytic functions.

47

48 **Introduction**

49 Separase (family C50, clan CD) is an evolutionary conserved cysteine protease participating in
50 the metaphase-to-anaphase transition and plant development (Liu & Makaroff, 2006; Moschou
51 & Bozhkov, 2012). In *Arabidopsis thaliana*, separase localizes to microtubules (Moschou *et*
52 *al.*, 2016a), the plasma membrane and the endosomal compartment *trans*-Golgi Network
53 (TGN)(Moschou *et al.*, 2013), which acts as a hub for protein vesicle trafficking.

54 Since loss-of-function *Arabidopsis* separase mutants are embryo lethal (Liu &
55 Makaroff, 2006), the roles of separase beyond cell division are studied by the conditional
56 temperature-sensitive loss-of-function allele *RADIALLY SWOLLEN 4* (*rsw4*). The *rsw4*
57 mutation renders separase unstable at 28°C (Wu *et al.*, 2010; Yang *et al.*, 2011; Moschou *et*
58 *al.*, 2016a). *Rsw4* shows root phenotypes reminiscent of compromised auxin distribution, with
59 perturbed gravitropism, cell expansion and overall development (Moschou *et al.*, 2013).
60 Proteolytic activity of separase is indispensable in development since the proteolytic inactive
61 separase mutant could not rescue *rsw4* defects. Yet, the proteolytic targets of separase remain
62 obscure.

63 Implementation of positional proteomics is the most direct method for unbiased
64 identification of protease substrates (Plasman *et al.*, 2013). When sampling complex
65 proteomes, protease substrates can be identified by exploiting the chemical reactivity of the
66 alpha-amino groups. Such newly introduced α -amino groups are typically referred to as neo-
67 N-termini (neo-Nt). The N-terminal COmbined FRActional DIagonal Chromatography
68 technology (COFRADIC; (Gevaert *et al.*, 2003) depletes non-Nt-peptides, thereby enriches for
69 Nt-peptides and further allows the specific identification of neo-Nt through a combination of
70 stable isotope labelling of neo-Nt, tandem mass spectrometry and bioinformatics.

71 Here we used COFRADIC to identify potential separase substrates that may allow
72 delineating new signalling pathways relevant to organ growth and development. By contrasting
73 the proteolytic landscape of wild-type (WT) and *rsw4* we infer potential proteolytic targets
74 relevant to vesicular trafficking, lipid signaling and root growth control. We succinctly discuss
75 the most relevant identified proteins and suggest potential molecular mechanisms for further
76 exploration.

77

78 **Results and Discussion**

79 *Inducible depletion of separase phenocopies rsw4 PIN2 polarity defects*

80 A potent readout for vesicular trafficking defects and early events imposed by the absence of
81 *rsw4* is the mis-localization of the auxin efflux carrier PINFORMED2 (PIN2) in root cortex

82 cells, responsible for auxin flow maintenance (Moschou *et al.*, 2013). Depletion of separase in
83 *rsw4* causes PIN2 localization switch from the proper rootward to the shootward side of the
84 plasma membrane in *rsw4* root cortex cells at the restrictive temperature. This PIN2
85 localization switch correlates with the reduced activity of a GNOM-related vesicular trafficking
86 pathway in *rsw4*. A functional GNOM-related pathway requires proteolytic cleavage of an as
87 yet unknown substrate(s) by separase, since the protease-dead allelic variant of separase could
88 not complement PIN2 localization defects of *rsw4* (Liu & Moschou, 2017).

89 We have established that treatment of *rsw4* seedlings for up to 24 h at the restrictive
90 temperature (28°C) disrupts separase activity and causes vesicular trafficking defects, but does
91 not compromise the rate and pattern of cell division and the identity of root cells (Moschou *et*
92 *al.*, 2013). We argue that this experimental setup enables to study roles of separase beyond its
93 mitotic role (Moschou *et al.*, 2016b). Note that a temperature of 28°C falls within the
94 physiological temperature range for Arabidopsis growth (Faden *et al.*, 2016). Yet, to ensure
95 that the *rsw4*-mediated effect in PIN2 polarity is not due to the temperature shift, we surveyed
96 PIN2 polarity in dexamethasone inducible RNAi lines of separase (DEX:ESP-RNAi)
97 expressing PIN2 under its native promoter (Moschou *et al.*, 2013)(**Fig. 1**). We observed PIN2
98 polarity loss in the DEX:ESP-RNAi lines already 12 h after dexamethasone application. Yet,
99 no effect was observed in the corresponding WT plants expressing PIN2 after dexamethasone
100 application (data not shown). These results suggests that the PIN2 localization switch does not
101 depend on temperature and therefore our experimental setup can be used to infer proteolytic
102 targets of separase.

103

104 *Systematic characterization of root tip N-terminomes*

105 Proteins are always synthesized with methionine (iMet) as the first Nt residue even when a
106 non-canonical translation initiation codon (i.e. non-AUG) is used. However, largely depending
107 on the nature of the second amino acid residue, this first iMet is often cleaved from mature
108 proteins by the N-terminal Met excision (NME) pathway through the Met aminopeptidase
109 (MAP)(Bonissone *et al.*, 2013). The N-terminome consists of all peptides that possess mature
110 protein Nt (\pm iMet) and neo-Nt that are proxies of *in vivo* proteolytic events.

111 To gain insights into the proteolytic landscape of root cells we analysed the *in vivo* N-
112 terminomes of root tips from 7-d-old seedlings of WT and *rsw4* plants grown at the restrictive
113 temperature for 24 h by a modified version of COFRADIC (**Materials and Methods** and **Fig.**
114 **2A, B**). COFRADIC also enables the identification of sequences spanning the scissile peptidic
115 bonds (Vandekerckhove *et al.*, 2004; Stes *et al.*, 2014). The root tip proteomes of WT and *rsw4*

116 were labelled with N-hydroxysuccinimide esters of either light (WT) or heavy (*rsw4*) isotopic
117 variants of butyric acid to mass tag both Nt arising from translation and neo-Nt. The differential
118 mass tagging of Nt (heavy versus light) enabled us to determine the proteome origin (*rsw4* or
119 WT, respectively) of each labelled peptide.

120 To identify translational Nt (peptides containing either the iMet or the 2nd amino acid
121 residue of the protein), we filtered-out peptides carrying neo-Nt (peptides containing Nt beyond
122 the 2nd residue). Out of the total number of 6,974 peptides identified (all present in both
123 genotypes with one exception discussed later), 2,840 possessed translationally yielded Nt
124 converging to 1,057 proteins (**File S1**). Out of 149 unique proteins retaining iMet, 58 proteins
125 had as 2nd residue glutamate (E), 30 aspartate (D) and 20 lysine (K) (E>D>K>>X) (**Fig. 3A**),
126 suggesting that residues with sufficiently large gyration radius block MAP activities (Van
127 Damme *et al.*, 2011; Van Damme *et al.*, 2012). Protein species devoid of iMet showed strong
128 preference for alanine (A; 29%) and serine (S; 11%) at the 2nd position (P1'; P1^{iMet}-P1'-P2'-
129 ...-Pn')(**Fig. 3A**). The functional importance of the 2nd residue can be related to the efficiency
130 of MAP to remove the iMet residue (Shemesh *et al.*, 2010). We thus confirm here that A and
131 S residues are among the most preferred ones in the P1' position of MAP substrates in root tip
132 cells (Frottin *et al.*, 2006).

133

134 *Acetylation of native Nt in root tips confirms previous studies and adds to the known plastid*
135 *types capable of N-terminal acetylation*

136 The exposed Nt of proteins is one of the major determinants of protein stability/half-life and
137 certain residues, when exposed at the Nt of a protein, act as triggers for degradation and are
138 therefore called “N-degrons” (Bachmair *et al.*, 1986). Nt-acetylation (Nt-ace) can target
139 proteins for degradation via a branch of the N-end rule pathway (Hwang *et al.*, 2010). Nt-ace
140 of nascent polypeptides is carried out by N- α -acetyltransferases (NATs) (reviewed in (Gibbs,
141 2015). Nt-ace typically occurs co-translationally, and, in contrast to lysine (K) acetylation, it
142 seems irreversible. Residues that are acetylated following iMet excision can also act as Nt-ace-
143 degrons when they are not shielded by correct protein folding and/or assembled into oligomeric
144 complexes. In this way, the acetylation-mediated N-end rule plays important roles in general
145 protein quality control.

146 Between 70 and 90% of eukaryotic proteins carrying Nt-ace and iMet-ace can be
147 targeted for degradation when followed by a bulky residue (e.g. tryptophan; W) (Zhang *et al.*,
148 2015). Out of 2,840 Nt peptides identified 2,067 were *in vivo* acetylated (72%), with 496
149 carrying iMet-ace (24% of Nt-ace and only 17% of all characterized Nt) (**Fig. 3B**). The majority

150 of experimentally identified Nt-ace (76%) are acetylated after removal of the iMet, displaying
151 at the 2nd position A>S>threonine (T)>>G (**Fig. 3C**). Notably, a similar pattern of acetylation
152 affinity for the 2nd Nt residue has been reported for humans and Arabidopsis leaves (Linster *et*
153 *al.*, 2015). Interestingly, we identified one neo-Nt carrying acetylation. Manual examination of
154 this peptide showed that it corresponds to the mature form of the plastid protein CUTA which
155 carries a peptide leader (Burkhead *et al.*, 2003). This observation is consistent with previous
156 results demonstrating acetylation of chloroplastic proteins (Rowland *et al.*, 2015), extending
157 the Nt-ace for plastids, as well.

158

159 *Nt-acetylation is increased in rsw4*

160 The log₂ ratios of light (WT) to heavy (*rsw4*) signals for all identified peptides were calculated
161 with the Mascot Distiller software. The standard deviation of these values for all the peptides
162 (according to the Huber-scale estimator (Foyn *et al.*, 2013)) was 0.39 with the median very
163 close to *zero* (0.09; **File S2**). These data suggest that the proteome of *rsw4* shows specific
164 changes rather than pleiotropic redistributions and therefore represents an excellent model for
165 the study of targeted proteomic changes.

166 In WT, 25 acetylated peptides (from 5 proteins) carrying iMet were significantly
167 enriched (5 proteins; 0.5>log₂), in contrast to 61 acetylated peptides (20 proteins) enriched in
168 *rsw4* (**Fig. 3D**). After the removal of the iMet, 1,567 peptides were acetylated of which 105
169 (19 proteins) were enriched in WT and as many as 359 (20 proteins) enriched in *rsw4*. These
170 data point to an increased accumulation of proteins carrying Nt-ace in *rsw4* root cells, which
171 can be a result of either the enhancement of the acetylation pathway or the abrogation of a
172 proteolytic machinery normally degrading these proteins.

173 In plants, Nt-ace is indispensable since NatA loss-of-function mutant is embryo lethal
174 (Linster *et al.*, 2015). Furthermore, the Nt-ace of SUPPRESSOR OF NPR1, CONSTITUTIVE
175 1 (SNC1) is important for plant immunity (Xu *et al.*, 2015). A specific branch of the N-end
176 rule pathway known as the acetylation N-end rule, targets Nt-ace as degrons and send them for
177 degradation by the proteasome (Liu & Moschou, 2017) and references therein). In yeast, two
178 E3 ligases that recognize Nt-ace-degrons were identified: the ER-associated DOA10/TEB4 and
179 cytosolic NOT4 (Lee *et al.*, 2016). Furthermore, a link between anaphase and protein
180 acetylation was suggested in yeast (Van Damme *et al.*, 2011). Whether separase crosstalks with
181 the N-end rule pathway and whether Nt-ace impinges on chromosomal segregation in plants
182 merits further investigation. It is not surprising however, that separase-mediated limited

183 proteolysis could crosstalk with digestive proteolytic pathways, as it has been recently
184 discussed (Minina, E.A. *et al.*, 2017).

185

186 *Identification of neo-Nt peptides in root proteomes and thus potential targets of separase*

187 To identify neo-Nt, i.e. the proxies for proteolytic cleavage, we applied the following filtering
188 criteria: i) positive selection of peptides with butyrylated Nt and ii) exclusion of butyrylated
189 iMet and 2nd residues of the protein. Following filtering, we identified 247 neo-Nt peptides
190 corresponding to 48 unique proteins (**File S1**). The preferable P1' residue of neo-Nt was S,
191 followed by T, A, and E (**Fig. 3E**).

192 Next, we focused on two classes of peptides: the significantly enriched neo-Nt peptides
193 in WT or *rsw4* (based on the labelling used). As the former might also appear because of
194 differential protein levels in the input proteomes, we scanned the data for the corresponding
195 precursor protein Nt or other neo-Nt peptides from these precursor proteins. We expected to
196 deal with three different scenarios of mass spectroscopy results. First, a specific neo-Nt peptide
197 is present in greater amounts in WT indicating potential separase-mediated (direct or indirect)
198 proteolytic event. Second, a neo-Nt peptide is present in both samples, but in a significantly
199 greater amount in *rsw4*. This scenario would indicate that the corresponding protein was
200 cleaved at the specified site by a protease, which was up/mis-regulated in *rsw4* or that the
201 protein fragment was less stable in WT. Third, the neo-Nt peptide are in equal amounts in both
202 samples, indicating that this cleavage event reflects a general metabolic process not affected
203 by separase depletion.

204 With the exception of the AT1G79320 (METACASPASE6) for which a neo-Nt was
205 identified only in *rsw4* (removal of a 10 kDa Nt fragment), and may reflect the deregulated
206 expression of this gene, all other neo-Nt-containing peptides were present in both WT and *rsw4*
207 (**File S1**). Nine neo-Nt of proteins were preferentially overrepresented in WT, while four in
208 *rsw4* (**Table 1**). Most of the cleavage events in the identified proteins occurred in coils or α -
209 helices (**Fig. 4**), a result consistent with previous findings in non-plant organisms (Timmer *et*
210 *al.*, 2009).

211 Interestingly, neo-Nt corresponding to the V-ATPase E1, H⁺-ATPases, Annexin 1
212 (increased in WT) and the SYNTAXIN 71 (SYP71; increased in *rsw4*) were the most striking
213 proteins relevant to the vesicular trafficking and auxin defects observed in *rsw4*. Annexin 1
214 and H⁺-ATPases, are plasma membrane proteins (Baucher *et al.*, 2011; Haruta *et al.*, 2015),
215 while the V-ATPase E1 localizes at the tonoplast and the TGN (Strompen *et al.*, 2005;
216 Schumacher & Krebs, 2010). Interestingly, separase localizes at the plasma membrane and

217 TGN at least transiently (Moschou *et al.*, 2013). We should note that for the two H⁺-ATPases
218 (as well as the identified oxygenase) we could not ascribe additional peptides except the
219 identified neo-Nt and therefore, they could be simply more abundant in WT.

220 In plants, V-ATPase activity acidifies the TGN and the vacuole (Strompen *et al.*, 2005;
221 Schumacher & Krebs, 2010). In mammalian cells, separase depletion leads to a decrease in
222 constitutive protein secretion as well as endosomal receptor recycling and degradation (Bacac
223 *et al.*, 2011). Depletion of separase results in increased vesicular pH mediated by V-ATPase
224 inhibition. It is thus reasonable to assume that plant separase may also regulate the acidification
225 of vesicles by modulating the V-ATPase activity.

226 The H⁺-ATPases (AHA) regulate cellular acidification and cell expansion by building
227 a proton gradient across the plasma membrane. Downregulation of AHA activity occurs after
228 treatment of plants with the growth inhibitory peptide, RALF, leading to the inhibition of cell
229 expansion (Haruta *et al.*, 2014). Processing might be a complementary mechanism to control
230 the activity of AHA proteins. Plants with a hyperactive allele of AHA2 (*ost2*) show abscisic
231 acid insensitivity and drought sensitivity (Merlot *et al.*, 2007). Furthermore, evidence suggest
232 a crosstalk between auxin signalling and acidification that involves the activation of AHA in
233 Arabidopsis roots (Fendrych *et al.*, 2016). A more complete understanding of hprocessing may
234 control AHA activity will provide new prospects for improving plant growth and drought
235 tolerance.

236 Annexin 1 (ANN1) is a root-specific annexin regulating root length via sensing pH-
237 dependent channel activity (Gorecka *et al.*, 2007). In pea (*Pisum sativum*) an ANN1 homologue
238 can also redistribute in response to gravistimulation (Clark *et al.*, 2000). In maize cells, other
239 annexins are known to stimulate Ca²⁺-dependent exocytosis (Carroll *et al.*, 1998). In animal
240 cells, cleavage of ANN1 at the N-terminus by calpain protease mediates the secretory processes
241 by modifying either requirements for Ca²⁺ or ANN1 efficacy in membrane binding, vesicle
242 aggregation or endocytic processing (Barnes & Gomes, 2002; Sugimoto *et al.*, 2016). Other
243 annexins, e.g. A2, is a Ca²⁺-, actin-, and lipid-binding protein mediating the formation of lipid
244 microdomains required for the structural and spatial organization of fusion sites at the plasma
245 membrane (Gabel *et al.*, 2015). It is tempting to speculate that separase may regulate the
246 activity of ANN1 by modifying its requirement for Ca²⁺. Interestingly, the Arabidopsis
247 separase has an EF-hand, responsible for Ca²⁺ binding.

248 The identified neo-Nt of the cytoplasmic Acyl-CoA-binding protein 4 (ACBP4) is
249 preferentially enriched in WT (**Table 1**). ACBP4 is involved in the transport of lipids ($C \geq 20$)
250 to the plasma membrane for the biosynthesis of surface lipids such as wax and cutin (Du *et al.*,

251 2016). Depletion of AtACBP4 in Arabidopsis resulted in decreases in galactolipids and
252 phospholipids, suggesting its role in membrane lipid biosynthesis, as well as diminished
253 capability in the generation of signals such as salicylate for induction of systemic acquired
254 resistance. It is yet unclear what could be the role of ACBP4 processing but may lead to protein
255 activity modulation. A reduced activity of ACBP4 in *rsw4* could compromise lipid signalling
256 that could contribute to the observed phenotypes.

257 The product of PROPEP7 (**Table 1**; enriched in WT) is a member of the PROPEP
258 family of Damage Associated Molecular Pattern (DAMP) elicitor peptides. The cleavage on
259 the PROPEP7 is interesting, since it corresponds to the predicted cleavage site that will release
260 the Pep7 elicitor peptide, but has never been experimentally shown (Bartels & Boller, 2015).
261 Furthermore, this family is believed to have extended functionalities beyond wounding and
262 immunity, potentially in growth and development (Bartels & Boller, 2015). In fact,
263 overexpression of PROPEP1 leads to larger root system in Arabidopsis (Huffaker *et al.*, 2006).
264 Interestingly, the identified cleavage event enriched in *rsw4* on Chaperonin 60 beta may also
265 be involved in pathogen resistance (**Table 1**). The corresponding mutant, *Arabidopsis lesion*
266 *initiation 1 (len1)*, develops necrotic lesions which may activate systemic acquired resistance
267 (Ishikawa *et al.*, 2003), without pathogen attack (Ishikawa, 2005).

268 The peroxidase PRX34 was found at significantly higher levels in *rsw4* (both neo-Nt
269 and internal peptides). PRX34 is an apoplastic reactive oxygen species (ROS) generator
270 involved in resistance to pathogens in Arabidopsis (Daudi *et al.*, 2012) and also root
271 development through a genetic interaction with the mitogen-activated protein kinase 6
272 (MAPK6) (Han *et al.*, 2015). Interestingly, *PRX34* mutants show larger leaves than WT.
273 Similarly, oxidases in the apoplast of tobacco plants modulate resistance to pathogens and plant
274 development in a pathway that involves ROS-MAPKs (Moschou *et al.*, 2008; Moschou *et al.*,
275 2009; Tisi *et al.*, 2011; Gemes *et al.*, 2016). We assume that it is unlikely that PRX34 is a direct
276 separase target considering PRX34 localization in the apoplast, but its deregulation is rather an
277 indirect effect.

278 The Qb-SNARE SYP71 (enriched in *rsw4*) is part of a bigger family of proteins
279 mediating vesicular fusion (El Kasmi *et al.*, 2013). Together with Qb-SNARE NPSN11 and
280 VAMP721,722 the SYP71 forms a tetrameric KNOLLE-containing complex. KNOLLE
281 mediates vesicular trafficking during Arabidopsis cytokinesis and its targeting to the
282 cytokinetic apparatus known as cell plate is compromised in *rsw4* (Moschou *et al.*, 2013).
283 Hence, a plausible scenario is that SYP71 is preferentially degraded in *rsw4*, an event which
284 may impact vesicular fusion. It is highly likely that vesicular fusion is compromised in the

285 absence of separase as it has been shown in Arabidopsis (Moschou *et al.*, 2013) and *C. elegans*
286 (Bembenek *et al.*, 2010; Mitchell *et al.*, 2014).

287 Finally, SPATULA is a negative (neo-Nt increased in WT), while KLU (neo-Nt
288 increased in *rsw4*) a positive cell division regulator (Alvarez & Smyth, 1999; Heisler *et al.*,
289 2001; Anastasiou *et al.*, 2007; Ichihashi *et al.*, 2010; Josse *et al.*, 2011; Makkena & Lamb,
290 2013). SPATULA is a transcription factor required for specification of carpel and valve tissues
291 by restricting cell division. The corresponding mutants show enhanced root and leaf growth.
292 KLU produces an as yet unknown mobile signal with cell division promoting properties. KLU
293 is involved in generating a mobile growth signal distinct from the classical phytohormones that
294 defines primordium size.

295

296 *Consensus cleavage sites of substrates enriched in wild-type and thus potential separase*
297 *targets*

298 Using iceLogo, we inspected the amino acid residues at the prime (P') and nonprime (P)
299 substrate positions and analysed the frequencies of specific residues after statistical correction
300 by means of the natural occurrence of amino acids in Arabidopsis proteins (Colaert *et al.*,
301 2009). Unlike what has been described for kleisin motifs cleaved by separase, our data do not
302 show specificity of Arabidopsis separase against EXXR (X, any residue) sequence (Sullivan *et al.*
303 *et al.*, 2004; Lin *et al.*, 2016) (**Fig. 5**). This finding suggests that either not all identified substrates
304 are direct targets of separase or that separase in plants has evolved broader cleavage specificity.
305 We should note that so far sequence specificity for separase in non-plants has been deduced
306 from cleavage sites on only few proteins related to cell division, i.e. SLK19 and kleisins and
307 may not reflect the general specificity of separases. Noteworthy, the kleisins in plants are a
308 multimeric gene family (da Costa-Nunes *et al.*, 2006; Ma *et al.*, 2016; Minina, E. A. *et al.*,
309 2017). Hence, plant separases may have adapted to the expansion of plant kleisins by adjusting
310 accordingly their substrate recognition repertoire.

311

312 **Conclusion**

313 We previously established a role for separase in controlling vesicular trafficking and plant
314 development (Moschou *et al.*, 2016a). Likewise, *C. elegans* separase is required for secretion
315 of Rab11-positive vesicles, and in human cells separase controls fusion and acidification of
316 vesicles (Bembenek *et al.*, 2010; Bacac *et al.*, 2011; Mitchell *et al.*, 2014). Interestingly, fusion
317 of vacuolar membranes in yeast requires proteasomal degradation of ubiquitinated Ypt7, a
318 yeast homolog of Rab7 GTPase (Kleijnen *et al.* 2007). Ubiquitination may also regulate

319 membrane fusion events that reassemble fragmented organelles after mitosis in mammalian
320 cells and vacuole-plasma membrane fusions in plant cells during plant immunity (Meyer &
321 Popp, 2008). Yet, the role of processing in vesicular trafficking remains unknown. Here, we
322 show that plant separase may be involved in the regulation of acidification and lipid signalling,
323 and we assign potential molecular targets for this function. Furthermore, we show that the
324 proteolytic landscape of *rsw4* mutants involves proteins that modulate resistance to pathogens,
325 cell expansion and cell division. This finding extends the possible functions of separase,
326 suggesting potential links of a core component of cell division and development to plant
327 immune responses.

328

329 **Materials and Methods**

330 *Plant Material and Growth Conditions*

331 *Arabidopsis thaliana* wild-type (WT) and *rsw4* plants in the Col-0 ecotype background were
332 grown on vertical plates containing half-strength Murashige and Skoog (MS) medium
333 supplemented with 1% (w/v) sucrose and 0.7% (w/v) plant agar, at 20°C (permissive
334 temperature) or 28°C (restrictive temperature), 16/8-h light/dark cycle, and light intensity 150
335 $\mu\text{E m}^{-2} \text{s}^{-1}$. The root swelling phenotype was observed in homozygous *rsw4* plants within 3 d
336 of incubation at 28°C. The dexamethasone RNAi lines are in Col-0 background and have been
337 previously described (Moschou *et al.*, 2013).

338 *A shortened N-terminal COFRADIC protocol: sample preparation*

339 Seedlings grown on MS plates with nylon filters (0.8 μm) were harvested and root tips were
340 collected after manual excision with a blade. Tips were snap frozen in liquid N_2 , and ground
341 into a fine powder with a mortar and pestle. Samples were prepared as previously described
342 (Tsiatsiani *et al.*, 2014). To achieve a total protein content of 1 mg, 0.2 g frozen ground tissue
343 was re-suspended in 1 mL of buffer containing 1% (w/v) 3-[(3-cholamidopropyl)-
344 dimethylammonio]-1-propanesulfonate (CHAPS), 0.5% (w/v) deoxycholate, 5 mM
345 ethylenediaminetetraacetic acid, and 10% glycerol in 50 mM HEPES buffer, pH 7.5, further
346 containing the suggested amount of protease inhibitors (one tablet/10 mL buffer) according to
347 the manufacturer's instructions (Roche Applied Science). The sample was centrifuged at
348 16,000g for 10 min at 4°C, and guanidinium hydrochloride was added to the cleared
349 supernatant to reach a final concentration of 4 M. Protein concentrations were measured with
350 the DC protein assay (Bio-Rad), and protein extracts were further modified for N-terminal
351 COFRADIC analysis as described previously (Staes *et al.*, 2011).

352 Col-0 (WT) primary amines were labelled with the N-hydroxysuccinimide (NHS) ester
353 of $^{12}\text{C}_4$ -butyrate and *rsw4* with NHS- $^{13}\text{C}_4$ -butyrate, resulting in a mass difference of
354 approximately 4 Da between light ($^{12}\text{C}_4$) and heavy ($^{13}\text{C}_4$) labelled peptides. After equal
355 amounts of the labelled proteomes had been mixed, tryptic digestion generated internal, non-
356 N-terminal peptides that were removed by strong cation exchange at low pH (Staes *et al.*,
357 2011). Due to the low amount of input material, the COFRADIC protocol was cut short after
358 the first reversed phase-high performance liquid chromatography (RP-HPLC) step and the
359 resulting 15 fractions were subjected immediately for identification by LC-MS/MS.

360 *Peptide Identification, and Quantification*

361 Samples were dissolved in 2% ACN, 0.1% TFA and subjected to ESI-MS/MS on a Q Exactive
362 Orbitrap mass spectrometer operated similarly as previously described with some
363 modifications (Stes *et al.*, 2014). Peptides were separated on a reverse phase column with a
364 linear gradient from 98% solvent A' (0.1% formic acid in water) to 40% solvent B' (0.1%
365 formic acid in water/acetonitrile, 20:80 (v/v) in 127 min at a flow rate of 300 nL/min. MS was
366 run in data-dependent, positive ionization mode, with the initial MS1 scan (400–2000 m/z;
367 AGC target of 3×10^6 ions; maximum ion injection time of 80 ms) acquired at a resolution
368 of 70 000 (at 200 m/z), which was followed by up to 10 tandem MS scans of the most abundant
369 ions at a resolution of 17 500 (at 200 m/z) according the following criteria: AGC target of $5 \times$
370 10^4 ions; maximum ion injection time of 120 ms; isolation window of 2.0 m/z; fixed first
371 mass of 140 m/z; underfill ratio of 1.2%; intensity threshold of 5×10^3 ; exclusion of
372 unassigned, 1, 5–8, >8 charged precursors; peptide match preferred; exclude isotopes, on;
373 dynamic exclusion time, 20 s. From the MS/MS data, Mascot Generic Files (mgf) were created
374 using the Mascot Distiller software (version 2.5.1.0, Matrix Science). Peak lists were then
375 searched using the Mascot search engine with the Mascot Daemon interface (version 2.5.1,
376 Matrix Science). Spectra were searched against the TAIR10 database. Mass tolerance on
377 precursor ions was set to 10 ppm (with Mascot's C13 option set to 1), and on fragment ions to
378 20 mmu. The instrument setting was on ESI-QUAD. Endoproteinase semi-Arg C/P was used
379 with one missed cleavage allowance, rather than trypsin, because cleavage after lysine residues
380 is abolished by side chain acylation. Variable modifications were set to pyroglutamate
381 formation of N-terminal glutamine and fixed modifications included methionine oxidation to
382 its sulfoxide derivative, S-carbamidomethylation of cysteine, and butyrylation ($^{12}\text{C}_4$ or $^{13}\text{C}_4$) of
383 the lysine side chain and peptide N-termini. Peptides with a score higher than the MASCOT
384 identity threshold set at 99% confidence were withheld. The Mascot Distiller Toolbox (version

385 2.5.1.0; Matrix Science) was used to quantify relative peptide abundance and in case of doubt
386 were manually curated (for example for singletons). MS data have been deposited to the
387 ProteomeXchange Consortium via the PRIDE (Vizcaino *et al.*, 2016).

388

389 **Supplemental Data**

390 **Supplemental File 1.** N-terminome of WT and *rsw4* Arabidopsis root tips.

391 **Supplemental File 2.** Variance distribution of peptides quantifications in WT and *rsw4*.

392

393 **Figure Legends**

394 **Figure 1. Temperature does not underpin the rootward-to-shootward PIN2 switch in**
395 ***rsw4*.**

396 DEX::hpRNAi-ESP plants expressing PIN2::PIN2-GFP were treated for 12 h with 2 μ M
397 dexamethasone (in DMSO) and observed using confocal microscopy. The root region and cells
398 observed (cortex and epidermis) are shown on the left. Representative images of an experiment
399 replicated three times. Scale bars, 5 μ m.

400

401 **Figure 2. The COFRADIC pipeline and the experimental setup.**

402 A. The COFRADIC steps are i) labelling: cysteine alkylation and N-trideutero-
403 acetylation (butylation); ii) trypsin digestion; ii) pyroQ removal and SCX at low pH.

404 B. WT and *rsw4* seedlings were exposed for 12 h at 28°C and their root tips were
405 harvested, their proteomes extracted and differentially labelled by staple isotopic tags and
406 analysed by COFRADIC (see also Materials and Methods).

407

408 **Figure 3. Gene ontology (GO) terms of identified root tip N-termini and residue**
409 **enrichments at position 2 of proteins with or without N-terminal methionine (iMet).**

410 A. Enriched residues of proteins with (top) or without iMet (bottom).

411 B. Distribution (%) of Nt-acetylated peptides lacking iMet (-iMet), with iMet (+iMet) and
412 peptides that were not Nt-acetylated (with or without iMet; -iMet or +iMet, respectively).

413 C. Acetylation specificity of peptides lacking iMet at the Nt (pooled data from WT and
414 *rsw4*).

415 D. Acetylation level of peptides in WT and *rsw4* expressed as a ratio between the
416 acetylated/non-acetylated forms of the same peptides.

417 E. P1'-P6' specificity of limited proteolysis in root tip cells.

418 **Figure 4. Domain architecture (left), cleavage sites and secondary structures (right) of the**
419 **neo-N-termini enriched in WT (above the dotted red line) or in *rsw4* (below the dotted**
420 **line).**

421 Domain architecture was defined by SMART (Letunic *et al.*, 2015). Secondary structures
422 represent predictions defined by YASPIN (Lin *et al.*, 2005). The only proteins identified from
423 these cleaved in loops are the V-ATPase E1 and PRX34.

424 **Figure 5. Icelogo showing the specificity of cleavage events enriched in WT.**

425

426 **References**

- 427 **Alvarez J, Smyth DR. 1999.** CRABS CLAW and SPATULA, two Arabidopsis genes that
428 control carpel development in parallel with AGAMOUS. *Development* **126**(11): 2377-
429 2386.
- 430 **Anastasiou E, Kenz S, Gerstung M, MacLean D, Timmer J, Fleck C, Lenhard M. 2007.**
431 Control of plant organ size by KLUH/CYP78A5-dependent intercellular signaling. *Dev*
432 *Cell* **13**(6): 843-856.
- 433 **Bacac M, Fusco C, Planche A, Santodomingo J, Demarex N, Leemann-Zakaryan R,**
434 **Provero P, Stamenkovic I. 2011.** Securin and Separase Modulate Membrane Traffic
435 by Affecting Endosomal Acidification. *Traffic* **12**(5): 615-626.
- 436 **Bachmair A, Finley D, Varshavsky A. 1986.** In vivo half-life of a protein is a function of its
437 amino-terminal residue. *Science* **234**(4773): 179-186.
- 438 **Barnes JA, Gomes AV. 2002.** Proteolytic signals in the primary structure of annexins. *Mol*
439 *Cell Biochem* **231**(1-2): 1-7.
- 440 **Bartels S, Boller T. 2015.** Quo vadis, Pep? Plant elicitor peptides at the crossroads of
441 immunity, stress, and development. *J Exp Bot* **66**(17): 5183-5193.
- 442 **Baucher M, Oukouomi Lowe Y, Vandeputte OM, Mukoko Bopopi J, Moussawi J,**
443 **Vermeersch M, Mol A, El Jaziri M, Homble F, Perez-Morga D. 2011.** Ntann12
444 annexin expression is induced by auxin in tobacco roots. *Journal of Experimental*
445 *Botany* **62**(11): 4055-4065.
- 446 **Bembenek JN, White JG, Zheng Y. 2010.** A role for separase in the regulation of RAB-11-
447 positive vesicles at the cleavage furrow and midbody. *Current Biology* **20**(3): 259-264.
- 448 **Bonissone S, Gupta N, Romine M, Bradshaw RA, Pevzner PA. 2013.** N-terminal protein
449 processing: a comparative proteogenomic analysis. *Mol Cell Proteomics* **12**(1): 14-28.
- 450 **Burkhead JL, Abdel-Ghany SE, Morrill JM, Pilon-Smits EA, Pilon M. 2003.** The
451 Arabidopsis thaliana CUTA gene encodes an evolutionarily conserved copper binding
452 chloroplast protein. *Plant Journal* **34**(6): 856-867.
- 453 **Carroll AD, Moyon C, Van Kesteren P, Tooke F, Battey NH, Brownlee C. 1998.** Ca²⁺,
454 annexins, and GTP modulate exocytosis from maize root cap protoplasts. *Plant Cell*
455 **10**(8): 1267-1276.
- 456 **Colaert N, Helsens K, Martens L, Vandekerckhove J, Gevaert K. 2009.** Improved
457 visualization of protein consensus sequences by iceLogo. *Nat Methods* **6**(11): 786-787.
- 458 **da Costa-Nunes JA, Bhatt AM, O'Shea S, West CE, Bray CM, Grossniklaus U, Dickinson**
459 **HG. 2006.** Characterization of the three Arabidopsis thaliana RAD21 cohesins reveals
460 differential responses to ionizing radiation. *Journal of Experimental Botany* **57**(4): 971-
461 983.
- 462 **Daudi A, Cheng ZY, O'Brien JA, Mammarella N, Khan S, Ausubel FM, Bolwell GP.**
463 **2012.** The Apoplastic Oxidative Burst Peroxidase in Arabidopsis Is a Major Component
464 of Pattern-Triggered Immunity. *Plant Cell* **24**(1): 275-287.
- 465 **Du ZY, Arias T, Meng W, Chye ML. 2016.** Plant acyl-CoA-binding proteins: An emerging
466 family involved in plant development and stress responses. *Prog Lipid Res* **63**: 165-
467 181.
- 468 **El Kasmi F, Krause C, Hiller U, Stierhof YD, Mayer U, Conner L, Kong L, Reichardt I,**
469 **Sanderfoot AA, Jurgens G. 2013.** SNARE complexes of different composition jointly
470 mediate membrane fusion in Arabidopsis cytokinesis. *Mol Biol Cell* **24**(10): 1593-1601.
- 471 **Faden F, Ramezani T, Mielke S, Almudi I, Nairz K, Froehlich MS, Hockendorff J, Brandt**
472 **W, Hoehenwarter W, Dohmen RJ, et al. 2016.** Phenotypes on demand via switchable
473 target protein degradation in multicellular organisms. *Nature Communications* **7**:
474 12202.
- 475 **Fendrych M, Leung J, Friml J. 2016.** TIR1/AFB-Aux/IAA auxin perception mediates rapid
476 cell wall acidification and growth of Arabidopsis hypocotyls. *Elife* **5**.

- 477 **Foyt H, Van Damme P, Stove SI, Glomnes N, Evjenth R, Gevaert K, Arnesen T. 2013.**
478 Protein N-terminal Acetyltransferases Act as N-terminal Propionyltransferases In Vitro
479 and In Vivo. *Molecular & Cellular Proteomics* **12**(1): 42-54.
- 480 **Frottin F, Martinez A, Peynot P, Mitra S, Holz RC, Giglione C, Meinnel T. 2006.** The
481 proteomics of N-terminal methionine cleavage. *Molecular & Cellular Proteomics*
482 **5**(12): 2336-2349.
- 483 **Gabel M, Delavoie F, Demais V, Royer C, Bailly Y, Vitale N, Bader MF, Chasserot-Golaz
484 S. 2015.** Annexin A2-dependent actin bundling promotes secretory granule docking to
485 the plasma membrane and exocytosis. *Journal of Cell Biology* **210**(5): 785-800.
- 486 **Gemes K, Kim YJ, Park KY, Moschou PN, Andronis E, Valassaki C, Roussis A,
487 Roubelakis-Angelakis KA. 2016.** An NADPH-Oxidase/Polyamine Oxidase Feedback
488 Loop Controls Oxidative Burst Under Salinity. *Plant Physiol* **172**(3): 1418-1431.
- 489 **Gevaert K, Goethals M, Martens L, Van Damme J, Staes A, Thomas GR,
490 Vandekerckhove J. 2003.** Exploring proteomes and analyzing protein processing by
491 mass spectrometric identification of sorted N-terminal peptides. *Nature Biotechnology*
492 **21**(5): 566-569.
- 493 **Gibbs DJ. 2015.** Emerging Functions for N-Terminal Protein Acetylation in Plants. *Trends
494 Plant Sci* **20**(10): 599-601.
- 495 **Han SA, Fang L, Ren XJ, Wang WL, Jiang J. 2015.** MPK6 controls H₂O₂-induced root
496 elongation by mediating Ca²⁺ influx across the plasma membrane of root cells in
497 Arabidopsis seedlings. *New Phytologist* **205**(2): 695-706.
- 498 **Haruta M, Gray WM, Sussman MR. 2015.** Regulation of the plasma membrane proton pump
499 (H⁺)-ATPase) by phosphorylation. *Curr Opin Plant Biol* **28**: 68-75.
- 500 **Haruta M, Sabat G, Stecker K, Minkoff BB, Sussman MR. 2014.** A peptide hormone and
501 its receptor protein kinase regulate plant cell expansion. *Science* **343**(6169): 408-411.
- 502 **Heisler MG, Atkinson A, Bylstra YH, Walsh R, Smyth DR. 2001.** SPATULA, a gene that
503 controls development of carpel margin tissues in Arabidopsis, encodes a bHLH protein.
504 *Development* **128**(7): 1089-1098.
- 505 **Huffaker A, Pearce G, Ryan CA. 2006.** An endogenous peptide signal in Arabidopsis
506 activates components of the innate immune response. *Proc Natl Acad Sci U S A*
507 **103**(26): 10098-10103.
- 508 **Hwang CS, Shemorry A, Varshavsky A. 2010.** N-terminal acetylation of cellular proteins
509 creates specific degradation signals. *Science* **327**(5968): 973-977.
- 510 **Ichihashi Y, Horiguchi G, Gleissberg S, Tsukaya H. 2010.** The bHLH transcription factor
511 SPATULA controls final leaf size in Arabidopsis thaliana. *Plant Cell Physiol* **51**(2):
512 252-261.
- 513 **Ishikawa A. 2005.** Tetrapyrrole metabolism is involved in lesion formation, cell death, in the
514 Arabidopsis lesion initiation 1 mutant. *Bioscience Biotechnology and Biochemistry*
515 **69**(10): 1929-1934.
- 516 **Ishikawa A, Tanaka H, Nakai M, Asahi T. 2003.** Deletion of a chaperonin 60 beta gene leads
517 to cell death in the Arabidopsis lesion initiation 1 mutant. *Plant Cell Physiol* **44**(3):
518 255-261.
- 519 **Josse EM, Gan Y, Bou-Torrent J, Stewart KL, Gilday AD, Jeffree CE, Vaistij FE,
520 Martinez-Garcia JF, Nagy F, Graham IA, et al. 2011.** A DELLA in disguise:
521 SPATULA restrains the growth of the developing Arabidopsis seedling. *Plant Cell*
522 **23**(4): 1337-1351.
- 523 **Lee KE, Heo JE, Kim JM, Hwang CS. 2016.** N-Terminal Acetylation-Targeted N-End Rule
524 Proteolytic System: The Ac/N-End Rule Pathway. *Mol Cells* **39**(3): 169-178.
- 525 **Letunic I, Doerks T, Bork P. 2015.** SMART: recent updates, new developments and status in
526 2015. *Nucleic Acids Res* **43**(Database issue): D257-260.

- 527 **Lin K, Simossis VA, Taylor WR, Heringa J. 2005.** A simple and fast secondary structure
528 prediction method using hidden neural networks. *Bioinformatics* **21**(2): 152-159.
- 529 **Lin Z, Luo X, Yu H. 2016.** Structural basis of cohesin cleavage by separase. *Nature*
530 **532**(7597): 131-134.
- 531 **Linster E, Stephan I, Bienvenut WV, Maple-Grodem J, Myklebust LM, Huber M,**
532 **Reichert M, Sticht C, Moller SG, Meinnel T, et al. 2015.** Downregulation of N-
533 terminal acetylation triggers ABA-mediated drought responses in Arabidopsis. *Nature*
534 *Communications* **6**: 7640.
- 535 **Liu C, Moschou PN. 2017.** Cutting in the middleman: hidden substrates at the interface
536 between proteases and plant development. *New Phytologist*.
- 537 **Liu Z, Makaroff CA. 2006.** Arabidopsis separase AESP is essential for embryo development
538 and the release of cohesin during meiosis. *Plant Cell* **18**(5): 1213-1225.
- 539 **Ma W, Schubert V, Martis MM, Hause G, Liu ZJ, Shen Y, Conrad U, Shi WQ, Scholz U,**
540 **Taudien S, et al. 2016.** The distribution of alpha-kleisin during meiosis in the
541 holocentromeric plant *Luzula elegans*. *Chromosome Research* **24**(3): 393-405.
- 542 **Makkena S, Lamb RS. 2013.** The bHLH transcription factor SPATULA is a key regulator of
543 organ size in Arabidopsis thaliana. *Plant Signal Behav* **8**(5): e24140.
- 544 **Merlot S, Leonhardt N, Fenzi F, Valon C, Costa M, Piette L, Vavasseur A, Genty B,**
545 **Boivin K, Muller A, et al. 2007.** Constitutive activation of a plasma membrane H(+)-
546 ATPase prevents abscisic acid-mediated stomatal closure. *Embo Journal* **26**(13): 3216-
547 3226.
- 548 **Meyer H, Popp O. 2008.** Role(s) of Cdc48/p97 in mitosis. *Biochem Soc Trans* **36**(Pt 1): 126-
549 130.
- 550 **Minina EA, Moschou PN, Bozhkov PV. 2017.** Limited and digestive proteolysis: crosstalk
551 between evolutionary conserved pathways. *New Phytologist*: In press.
- 552 **Minina EA, Reza SH, Gutierrez-Beltran E, Elander PH, Bozhkov PV, Moschou PN. 2017.**
553 The Arabidopsis homolog of *Scc4/MAU2* is essential for embryogenesis. *J Cell Sci*
554 **130**(6): 1051-1063.
- 555 **Mitchell DM, Uehlein-Klebanow LR, Bembenek JN. 2014.** Protease-Dead Separase Is
556 Dominant Negative in the *C. elegans* Embryo. *Plos One* **9**(9).
- 557 **Moschou PN, Bozhkov PV. 2012.** Separases: Biochemistry and function. *Physiol Plant*
558 **145**(1): 67-76.
- 559 **Moschou PN, Gutierrez-Beltran E, Bozhkov PV, Smertenko A. 2016a.** Separase Promotes
560 Microtubule Polymerization by Activating CENP-E-Related Kinesin Kin7.
561 *Developmental Cell* **37**(4): 350-361.
- 562 **Moschou PN, Paschalidis KA, Delis ID, Andriopoulou AH, Lagiotis GD, Yakoumakis DI,**
563 **Roubelakis-Angelakis KA. 2008.** Spermidine exodus and oxidation in the apoplast
564 induced by abiotic stress is responsible for H₂O₂ signatures that direct tolerance
565 responses in tobacco. *Plant Cell* **20**(6): 1708-1724.
- 566 **Moschou PN, Sarris PF, Skandalis N, Andriopoulou AH, Paschalidis KA, Panopoulos NJ,**
567 **Roubelakis-Angelakis KA. 2009.** Engineered polyamine catabolism preinduces
568 tolerance of tobacco to bacteria and oomycetes. *Plant Physiol* **149**(4): 1970-1981.
- 569 **Moschou PN, Savenkov EI, Minina EA, Fukada K, Reza SH, Gutierrez-Beltran E,**
570 **Sanchez-Vera V, Suarez MF, Hussey PJ, Smertenko AP, et al. 2016b.** EXTRA
571 SPINDLE POLES (Separase) controls anisotropic cell expansion in Norway spruce
572 (*Picea abies*) embryos independently of its role in anaphase progression. *New*
573 *Phytologist* **212**(1): 232-243.
- 574 **Moschou PN, Smertenko AP, Minina EA, Fukada K, Savenkov EI, Robert S, Hussey PJ,**
575 **Bozhkov PV. 2013.** The caspase-related protease separase (extra spindle poles)
576 regulates cell polarity and cytokinesis in Arabidopsis. *Plant Cell* **25**(6): 2171-2186.

- 577 **Plasman K, Van Damme P, Gevaert K. 2013.** Contemporary positional proteomics strategies
578 to study protein processing. *Curr Opin Chem Biol* **17**(1): 66-72.
- 579 **Rowland E, Kim J, Bhuiyan NH, van Wijk KJ. 2015.** The Arabidopsis Chloroplast Stromal
580 N-Terminome: Complexities of Amino-Terminal Protein Maturation and Stability.
581 *Plant Physiol* **169**(3): 1881-1896.
- 582 **Schumacher K, Krebs M. 2010.** The V-ATPase: small cargo, large effects. *Curr Opin Plant*
583 *Biol* **13**(6): 724-730.
- 584 **Shemesh R, Novik A, Cohen Y. 2010.** Follow the leader: preference for specific amino acids
585 directly following the initial methionine in proteins of different organisms. *Genomics*
586 *Proteomics Bioinformatics* **8**(3): 180-189.
- 587 **Staes A, Impens F, Van Damme P, Ruttens B, Goethals M, Demol H, Timmerman E,**
588 **Vandekerckhove J, Gevaert K. 2011.** Selecting protein N-terminal peptides by
589 combined fractional diagonal chromatography. *Nat Protoc* **6**(8): 1130-1141.
- 590 **Stes E, Laga M, Walton A, Samyn N, Timmerman E, De Smet I, Goormachtig S, Gevaert**
591 **K. 2014.** A COFRADIC protocol to study protein ubiquitination. *J Proteome Res* **13**(6):
592 3107-3113.
- 593 **Strompen G, Dettmer J, Stierhof YD, Schumacher K, Jurgens G, Mayer U. 2005.**
594 Arabidopsis vacuolar H⁺-ATPase subunit E isoform 1 is required for Golgi
595 organization and vacuole function in embryogenesis. *Plant Journal* **41**(1): 125-132.
- 596 **Sugimoto MA, Vago JP, Teixeira MM, Sousa LP. 2016.** Annexin A1 and the Resolution of
597 Inflammation: Modulation of Neutrophil Recruitment, Apoptosis, and Clearance. *J*
598 *Immunol Res* **2016**: 8239258.
- 599 **Sullivan M, Hornig NC, Porstmann T, Uhlmann F. 2004.** Studies on substrate recognition
600 by the budding yeast separase. *J Biol Chem* **279**(2): 1191-1196.
- 601 **Timmer JC, Zhu W, Pop C, Regan T, Snipas SJ, Eroshkin AM, Riedl SJ, Salvesen GS.**
602 **2009.** Structural and kinetic determinants of protease substrates. *Nat Struct Mol Biol*
603 **16**(10): 1101-1108.
- 604 **Tisi A, Federico R, Moreno S, Lucretti S, Moschou PN, Roubelakis-Angelakis KA,**
605 **Angelini R, Cona A. 2011.** Perturbation of polyamine catabolism can strongly affect
606 root development and xylem differentiation. *Plant Physiol* **157**(1): 200-215.
- 607 **Tsiatsiani L, Stael S, Van Damme P, Van Breusegem F, Gevaert K. 2014.** Preparation of
608 Arabidopsis thaliana seedling proteomes for identifying metacaspase substrates by N-
609 terminal COFRADIC. *Methods Mol Biol* **1133**: 255-261.
- 610 **Van Damme P, Hole K, Pimenta-Marques A, Helsens K, Vandekerckhove J, Martinho**
611 **RG, Gevaert K, Arnesen T. 2011.** NatF Contributes to an Evolutionary Shift in Protein
612 N-Terminal Acetylation and Is Important for Normal Chromosome Segregation. *Plos*
613 *Genetics* **7**(7).
- 614 **Van Damme P, Lasa M, Plevoda B, Gazquez C, Elosegui-Artola A, Kim DS, De Juan-**
615 **Pardo E, Demeyer K, Hole K, Larrea E, et al. 2012.** N-terminal acetylome analyses
616 and functional insights of the N-terminal acetyltransferase NatB. *Proc Natl Acad Sci U*
617 *S A* **109**(31): 12449-12454.
- 618 **Vandekerckhove J, Van Damme P, Staes A, Martens L, Van Damme J, Demol H, De**
619 **Groot S, Ghesquiere B, Timmerman E, Thomas G, et al. 2004.** COFRADIC (TM) :
620 A highly versatile and quantitative gel-free Proteome technology, suited for global
621 analysis of a variety of post-translational protein modifications. *Molecular & Cellular*
622 *Proteomics* **3**(10): S304-S304.
- 623 **Vizcaino JA, Csordas A, del-Toro N, Dianas JA, Griss J, Lavidas I, Mayer G, Perez-**
624 **Riverol Y, Reisinger F, Ternent T, et al. 2016.** 2016 update of the PRIDE database
625 and its related tools. *Nucleic Acids Res* **44**(D1): D447-456.

- 626 **Wu S, Scheible WR, Schindelasch D, Van Den Daele H, De Veylder L, Baskin TI. 2010.**
627 A conditional mutation in *Arabidopsis thaliana* separase induces chromosome non-
628 disjunction, aberrant morphogenesis and cyclin B1;1 stability. *Development* **137**(6):
629 953-961.
- 630 **Xu F, Huang Y, Li L, Gannon P, Linster E, Huber M, Kapos P, Bienvenut W, Polevoda**
631 **B, Meinnel T, et al. 2015.** Two N-terminal acetyltransferases antagonistically regulate
632 the stability of a nod-like receptor in *Arabidopsis*. *Plant Cell* **27**(5): 1547-1562.
- 633 **Yang XH, Boateng KA, Yuan L, Wu S, Baskin TI, Makaroff CA. 2011.** The Radially
634 Swollen 4 Separase Mutation of *Arabidopsis thaliana* Blocks Chromosome Disjunction
635 and Disrupts the Radial Microtubule System in Meicytes. *Plos One* **6**(4).
- 636 **Zhang H, Deery MJ, Gannon L, Powers SJ, Lilley KS, Theodoulou FL. 2015.** Quantitative
637 proteomics analysis of the Arg/N-end rule pathway of targeted degradation in
638 *Arabidopsis* roots. *Proteomics* **15**(14): 2447-2457.
- 639

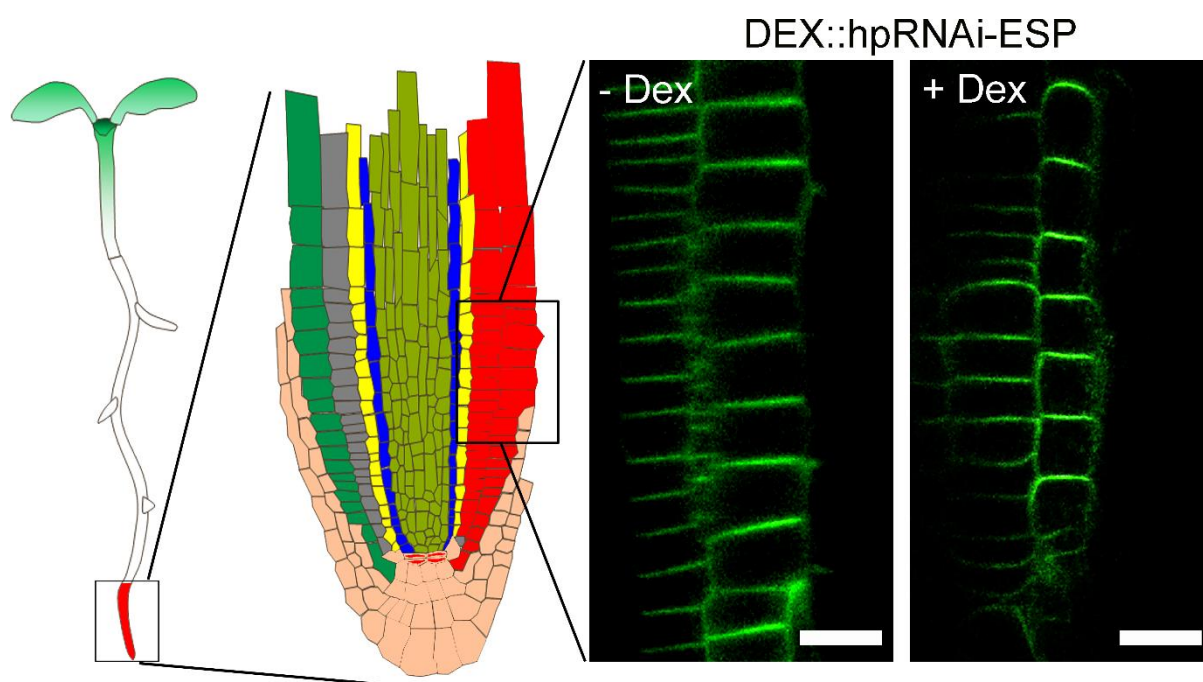
Table 1. Preferentially cleaved proteins (ratio >2) in WT and *rsw4* root tips. ¹Only neo-Nt peptides were identified; ²Non neo-Nt peptides were significantly increased in *rsw4*.

Accession	ID	Sequence	Ratio	Function
Preferentially cleaved in WT				
AT1G35720	Annexin 1	SKAQINATFNR	75,1	Calcium-dependent phospholipid binding
AT5G63400	Adenylate kinase 1	TVTQAEKLDMLKR	15,2	Nucleotide kinase activity
AT4G36930	SPATULA	TTTTTASLIGVHG	10,1	Cell division control
AT3G05420	Acyl-CoA binding protein 4	ATSGPAYPER	13,0	Acyl-CoA binding
AT2G17720	Oxygenase ¹	KSETSSGDEEGER	2,1	Modifies the extensin proteins in root hair cells
AT1G80660	H(+)-ATPase 9 ¹	EAQWAQAQR	2,1	ATPase, P-type, H+ proton pump
AT2G18960	H(+)-ATPase 1 ¹	ELSEIAEQAKR	2,0	ATPase, P-type, H+ proton pump
AT4G11150	V-ATP subunit E1	QDYEKKEKQADV	2,0	ATPase, V1/A1 complex, subunit E
AT5G09978	PROPEP7	SVVSGNVAAR	2,0	Plant immunity
Preferentially cleaved in <i>rsw4</i>				
AT1G13710	KLU ¹	VLAALAKR	1031,9	Positive regulation of cell proliferation
AT3G49120	Peroxidase PRX34 ²	SALVDFDLR	12,8	Unidimensional cell expansion
AT1G55490	Chaperonin 60 beta ¹	IVNDGVTVAR	10,2	SAR, suppression of protein aggregation.
AT3G09740	Syntaxin of plants 71 ¹	ATSDLKNTNVR	2,3	protein targeting to membrane, vesicle docking and fusion

640

641

642

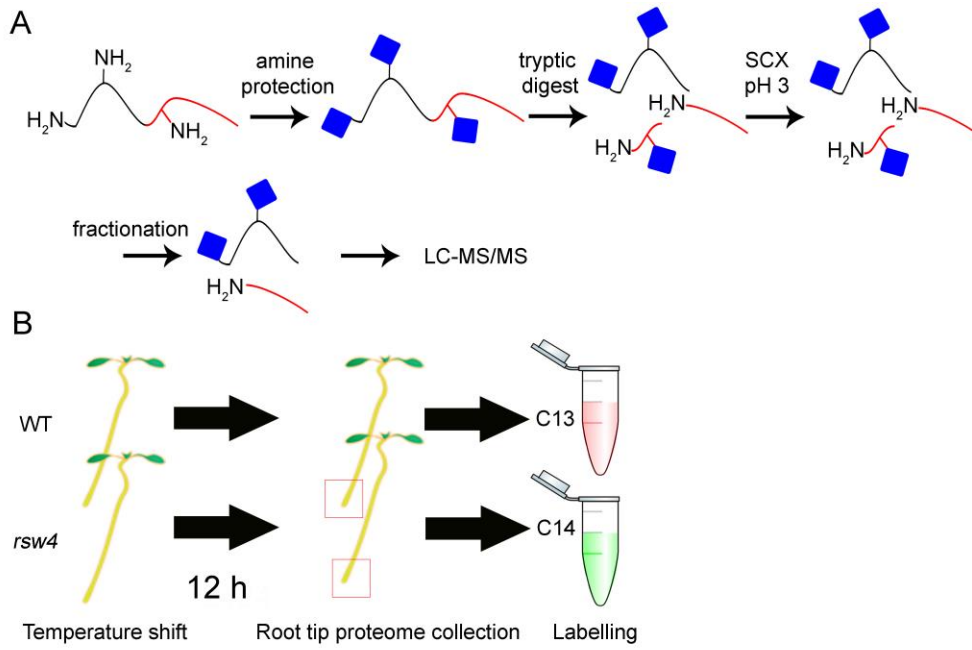


643

644

645

Figure 1

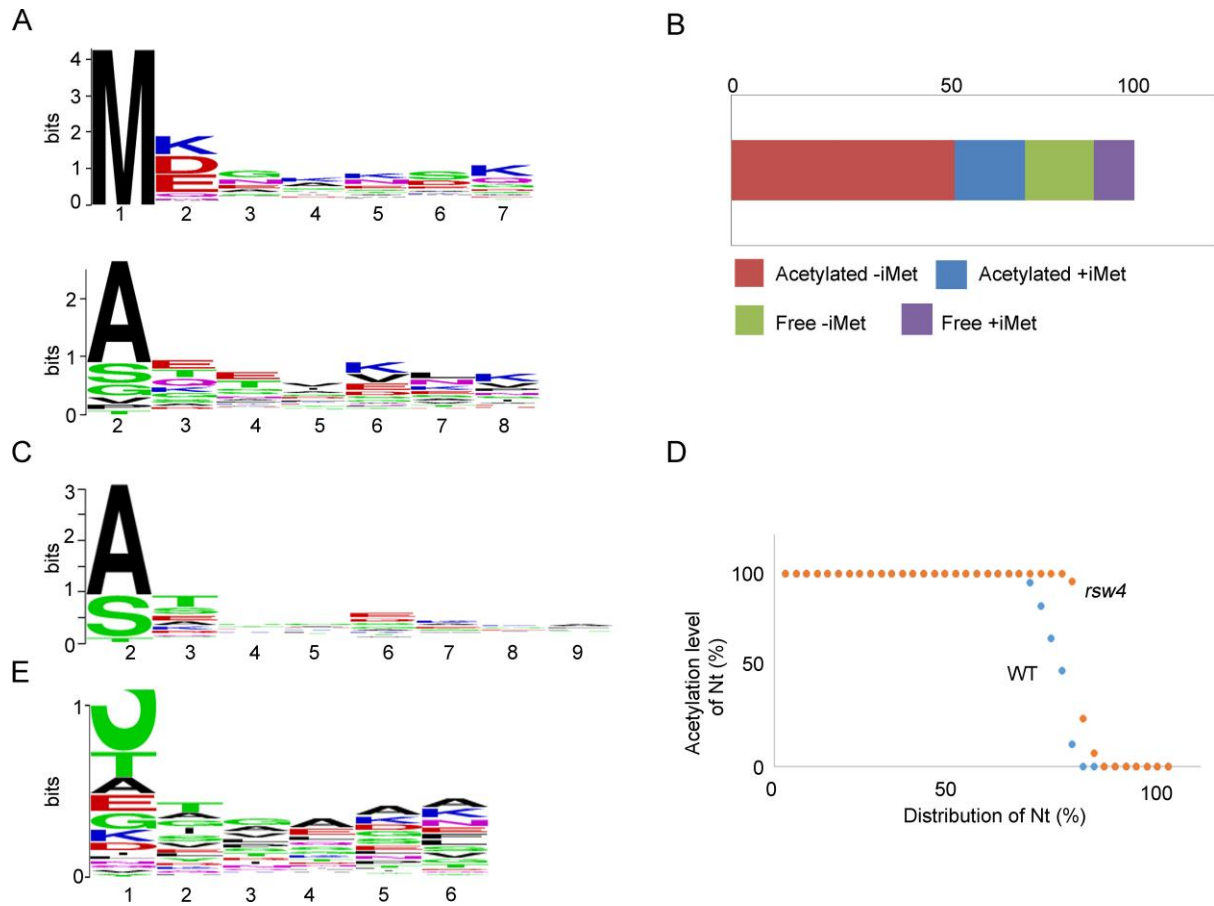


646

647

648

Figure 2



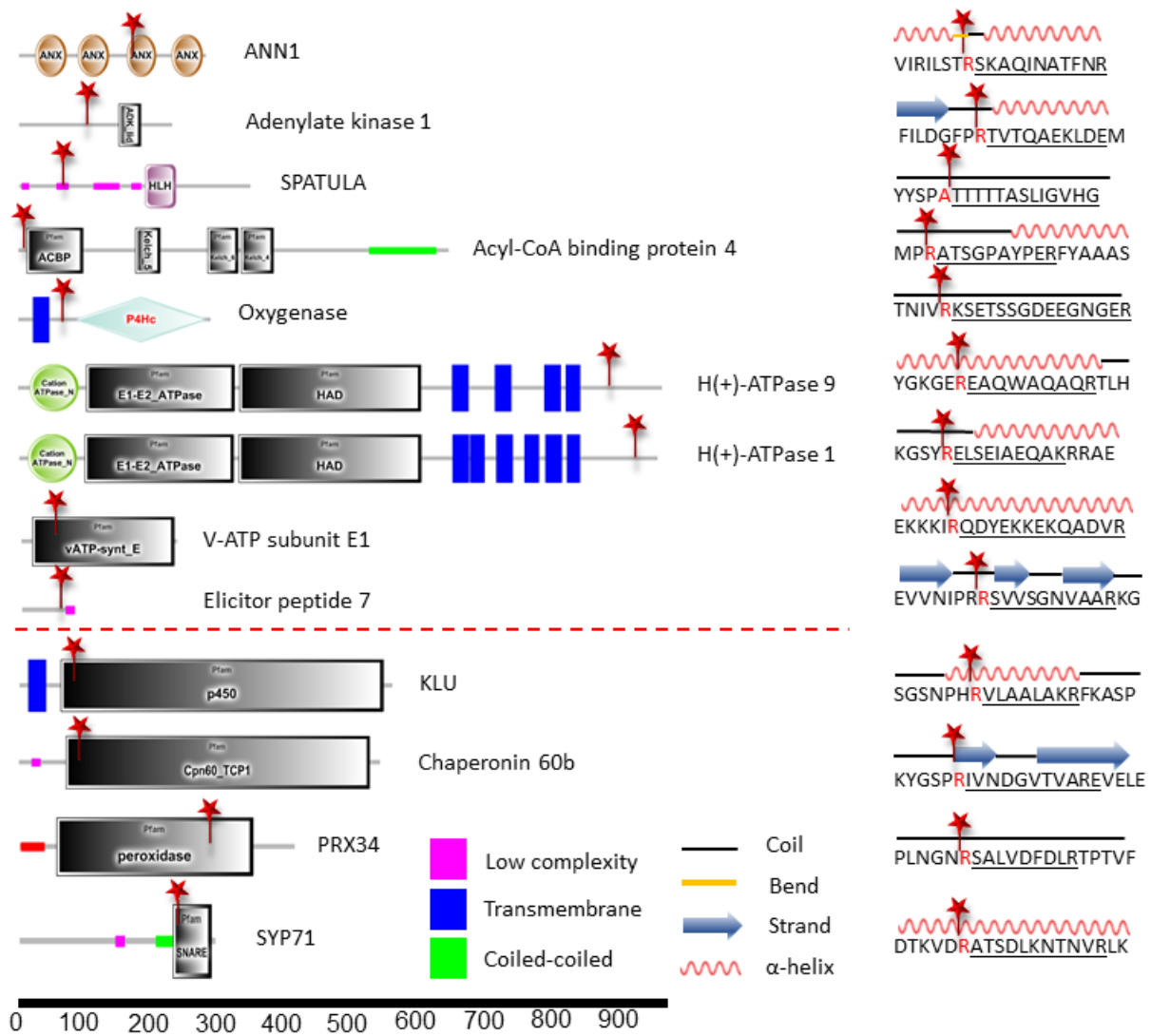
649

650

651

Figure 3

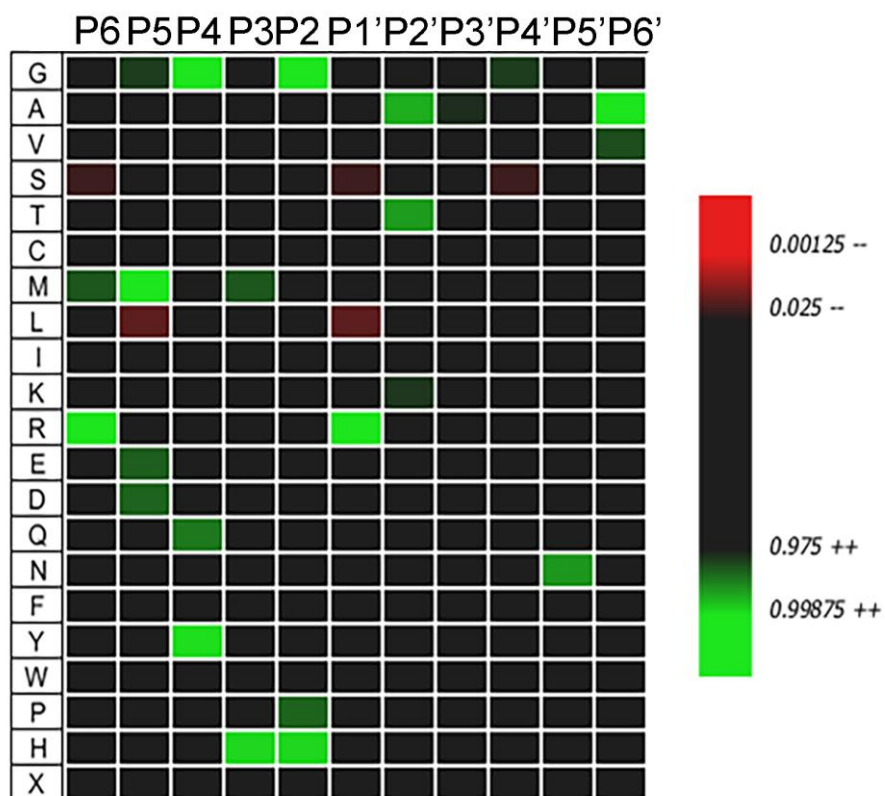
652



653

654

Figure 4



655

656

657

658

Figure 5